ScientificScholar®
Knowledge is power
Publisher of Scientific Journals

www.clinicalimagingscience.org

Journal of Clinical Imaging Science

Original Research

Dual-Energy Computed Tomography Lung in patients of Pulmonary Tuberculosis

Ahmad Umar Khan[1], Sachin Khanduri[1], Zikra Tarin[1], Syed Zain Abbas[1], Mushahid Husain[1], Anchal Singh[1], Poonam Yadav[1], Shreshtha Jain[1]

[1]Department of Radiodiagnosis, Era's Lucknow Medical College and Hospital, Sarfarazganj, Lucknow, Uttar Pradesh, India.

***Corresponding author:**
Sachin Khanduri,
Department of Radiodiagnosis,
Era's Lucknow Medical College
and Hospital, Sarfarazganj,
Lucknow - 226 016,
Uttar Pradesh, India.

drsachinrad@gmail.com

Received : 22 May 2020
Accepted : 21 June 2020
Published : 18 July 2020

DOI
10.25259/JCIS_78_2020

Quick Response Code:

ABSTRACT

Objectives: The objective of this study was to characterize findings of high-resolution computed tomography (HRCT) and dual-energy CT (DECT) (80 keV, 140 keV, and mixed) in pulmonary tuberculosis (TB) patients and to compare and correlate HRCT and DECT findings.

Material and Methods: This cross-sectional study was conducted on 67 patients of 18–65 years of age who were suspected cases of pulmonary TB with signs and symptoms of cough, fever, hemoptysis, sputum, night sweats, and weight loss with positive sputum AFB examinations/bronchoalveolar lavage. All the patients subjected to HRCT scan and followed with DECT scan. Comparison of various imaging techniques (DECT 80 keV, DECT 140 keV, and DECT mixed) with HRCT was done for detecting lung findings and data so obtained were subjected to statistical analysis.

Results: On comparing the various imaging techniques with HRCT for detecting consolidation, tree in bud pattern, cavitary lesions, ground-glass opacity, bronchiectasis, atelectasis, nodules, granuloma, peribronchial thickening, and fibrosis, the maximum agreement of HRCT was found with DECT 80 keV and minimum agreement was found with DECT 140 keV.

Conclusion: The study concluded that DECT 80 keV monochromatic reconstructions among 80 keV, mixed, and 140 keV monochromatic reconstructions in lung parenchyma window settings are a faster and better analytical tool for the assessment of findings of pulmonary TB when compared with HRCT.

Keywords: Dual-energy computed tomography, High-resolution computed tomography, Pulmonary tuberculosis

INTRODUCTION

Tuberculosis (TB) is an airborne infectious disease caused by *Mycobacterium tuberculosis* and is a major cause of morbidity and mortality, particularly in developing countries.[1-3] If TB is detected early and fully treated, people with the disease quickly become non-infectious and eventually cured. However, multidrug-resistant (MDR) and extensively drug-resistant TB, HIV-associated TB, and weak health systems are major challenges.[4]

India accounted for 26% of total cases of TB worldwide in 2012.[5] TB is one of the leading causes of mortality in India, killing two persons every 3 min, nearly 1000 every day.[6] A complete evaluation for TB must include a medical history, a chest radiograph, a physical examination, microbiologic smears, and cultures. It may also include a tuberculin skin test and a serologic test.[7]

The tuberculin skin test which has been used for years for the diagnosis of latent TB infection has many limitations, including false-positive test results in individuals who were vaccinated with bacilli Calmette-Guérin (BCG) and in individuals who have infections not related to *M. tuberculosis*. Culturing mycobacteria are mainly done on solid media, the Lowenstein–Jensen slope, or in broth media. These methods are slow, with cultures from microscopy-positive material taking from 2 to 4 weeks and for microscopy-negative material from 4 to 8 weeks. Chest X-ray is useful but is not specific for diagnosing pulmonary TB and can be normal even when the disease is present.[8] Therefore, it cannot provide a conclusive independent diagnosis and needs to be followed by sputum testing.

Computed tomography (CT) is more sensitive than chest radiography in the detection and characterization of both subtle localized or disseminated parenchymal disease and mediastinal lymphadenopathy.[9-12] High-resolution CT (HRCT) is a powerful and reliable investigation in the diagnosis of TB, when other means of diagnosis (e.g., culture and BAL) fail to settle the matter, are not available or time consuming.

Advances in technology such as quicker scan times, thin slices, and many reformat and 3D reconstructions have led to the revolutionization of the CT field. Dual-energy CT (DECT) is one of the most significant radiological developments in recent history. It creates improved contrasting image resolution by concurrently using scan data at two different X-ray tube energy levels – typically 80 kV and 140 kV. It's referred to as "dual energy" because it utilizes spectra of two photons; so, DECT is additionally mentioned as "spectral CT." Dual-energy CT offers exciting advanced and complex, but previously inaccessible applications with traditional single-energy CT technology. The potential edges of DECT embrace exaggerated detection and characterization of a lesion, near accurate staging, and analysis of treatment response, and reduction of artifacts, all at comparable or maybe reduced radiation dose.

MATERIAL AND METHODS

This cross-sectional study was conducted in the Department of Radio-Diagnosis, Era's Lucknow Medical College and Hospital, Lucknow, from January 2018 to November 2019. The study protocol was cleared for ethics by research institutional review board. This study addresses the optimal monochromatic keV level for lung parenchyma analysis in cases of pulmonary TB on routine DECT in comparison to HRCT.

Data collected included demographic information, clinical features, and laboratory findings. Written and informed consent from the patient and their relatives were taken. The ultimate unit of study was an adult patient of age group 18–65 years, sample size was 67. The clinical criteria for suspected cases of pulmonary TB were patients with signs and symptoms of cough, fever, hemoptysis, sputum, night sweats, and weight loss. Sputum smear microscopy, culture for AFB, and CXR posteroanterior (PA) view were the initial investigations performed in adults suspects.

All known and newly diagnosed cases of pulmonary TB on treatment, with or without positive chest radiograph findings, and sputum AFB who were willing to take part in study of any gender of age group 18–65 years with normal kidney function test were included in the study. A total of 67 patients attending the OPD and IPD in the department of pulmonary medicine, with the clinical criteria of pulmonary TB were interviewed and recruited. Patients allergic to contrast with lung pathology other than pulmonary TB who are immunocompromised or diagnosed with malignancy were excluded from the study. Initial detection of any pulmonary lesion was done by subjecting the patient to HRCT scan. HRCT scans were obtained on routine protocols. All the patients subjected to HRCT scan were followed with DECT scan.

Scan protocol

These patients underwent pulmonary DECT on a dual source CT scanner (Somatom Force scanner, Siemens Healthcare). Each scan was performed with a 512 × 512 matrix, 14 mm × 1.2 mm collimation, 50 mAs (effective) at 140 kV and 210 mAs (effective) at 80 kV, pitch of 0.5, and gantry rotation time of 0.33 s. Images from the lung apex to the costophrenic angles were acquired in a single breath hold in the craniocaudal direction. A power injector was used to administer 100 ml of iodine contrast material (iopromide, Ultravist 370) at a rate of 3.5 ml/with a fixed scan delay of 20 s.

Image generation

Two simultaneous helical scans were acquired with two tubes of 140 and 80 kV. The data from each tube were collected at the two independent tubes [A and B]. Weighted average images of approximately 120 keV were automatically generated from 140 and 80 keV images with a weighting factor of 1:4 [140:80]. Data from the 80 kV, 140 kV, and weighted average images were transferred to a workstation.

Image analysis

Images were analyzed on syngo workstation software. All the examinations were displayed with a lung parenchyma window with systematic multiplanar and 5 mm thickness maximum intensity projection reconstructions; for every patient, reader had to eventually designate which reconstruction

(i.e., keV level) offered the best diagnostic and image quality. Comparison of various imaging techniques (DECT 80 keV, DECT 140 keV, and DECT mixed) with HRCT was done for the assessment of pulmonary TB findings of consolidation [Table 1], tree in bud pattern [Table 2], cavity [Table 3], ground-glass opacity [Table 4], tractional bronchiectasis [Table 5], atelectasis [Table 6], ill-defined nodules [Table 7], calcified granuloma [Table 8], peribronchial thickening [Table 9], and fibrosis [Table 10].

Statistical analysis

Data entry was made in MS Office Excel software in codes and analysis was done by SPSS software® version 18.0.

Table 1: Comparison of various imaging techniques with HRCT For detecting consolidation.

Consolidation	HRCT		DECT 80 keV		DECT 140 keV		Mixed	
	No.	%	No.	%	No.	%	No.	%
Negative	39	58.2	40	59.7	44	65.7	42	62.7
Positive	28	41.8	27	40.3	23	34.3	25	37.3
Total	67	100.0	67	100.0	67	100.0	67	100.0
+ve % of HRCT			96.4		82.1		89.3	
Significance			χ^2=62.99, *P*<0.001		χ^2=48.78, *P*<0.001		χ^2=55.55, *P*<0.001	
Agreement			κ=0.969		κ=0.843		κ=0.907	

Table 2: Comparison of various imaging techniques with HRCT for detecting tree in bud pattern.

Tree in bud pattern	HRCT		DECT 80 keV		DECT 140 keV		Mixed	
	No.	%	No.	%	No.	%	No.	%
Negative	27	40.3	28	41.8	33	49.3	30	44.8
Positive	40	59.7	39	58.2	34	50.7	37	55.2
Total	67	100.0	67	100.0	67	100.0	67	100.0
+ve % of HRCT			97.5		85.0		92.5	
Significance			χ^2=62.99, *P*<0.001		χ^2=46.60, *P*<0.001		χ^2=55.78, *P*<0.001	
Agreement			κ=0.969		κ=0.820		κ=0.909	

Table 3: Comparison of various imaging techniques with HRCT for detecting cavity.

Cavity	HRCT		DECT 80 keV		DECT 140 keV		Mixed	
	No.	%	No.	%	No.	%	No.	%
Negative	40	59.7	40	59.7	44	65.7	42	62.7
Positive	27	40.3	27	40.3	23	34.3	25	37.3
Total	67	100.0	67	100.0	67	100.0	67	100.0
+ve % of HRCT			100.0		85.2		92.6	
Significance			χ^2=67.00, *P*<0.001		χ^2=51.89, *P*<0.001		χ^2=59.08, *P*<0.001	
Agreement			κ=1.000		κ=0.873		κ=0.937	

Table 4: Comparison of various imaging techniques with HRCT for detecting GGO.

GGO	HRCT		DECT 80 keV		DECT 140 keV		Mixed	
	No.	%	No.	%	No.	%	No.	%
Negative	45	67.2	46	68.7	48	71.6	46	68.7
Positive	22	32.8	21	31.3	19	28.4	21	31.3
Total	67	100.0	67	100.0	67	100.0	67	100.0
+ve % of HRCT			95.5		86.4		95.5	
Significance			χ^2=62.56, *P*<0.001		χ^2=54.25, *P*<0.001		χ^2=62.56, *P*<0.001	
Agreement			κ=0.966		κ=0.895		κ=0.966	

Table 5: Comparison of various imaging techniques with HRCT for detecting tractional bronchiectasis.

Traction bronchiectasis	HRCT		DECT 80 keV		DECT 140 keV		Mixed	
	No.	%	No.	%	No.	%	No.	%
Negative	48	71.6	49	73.1	50	74.6	50	74.6
Positive	19	28.4	18	26.9	17	25.4	17	25.4
Total	67	100.0	67	100.0	67	100.0	67	100.0
+ve % of HRCT			94.7		89.5		89.5	
Significance			χ^2=62.18, *P*<0.001		χ^2=57.55, *P*<0.001		χ^2=57.55, *P*<0.001	
Agreement			κ=0.963		κ=0.924		κ=0.924	

Table 6: Comparison of various imaging techniques with HRCT for detecting atelectasis.

Atelectasis	HRCT		DECT 80 keV		DECT 140 keV		Mixed	
	No.	%	No.	%	No.	%	No.	%
Negative	54	80.6	54	80.6	56	83.6	55	82.1
Positive	13	19.4	13	19.4	11	16.4	12	17.9
Total	67	100.0	67	100.0	67	100.0	67	100.0
+ve % of HRCT			100.0		84.6		92.3	
Significance			χ^2=67.00, *P*<0.001		χ^2=54.67, *P*<0.001		χ^2=60.72, *P*<0.001	
Agreement			κ=1.000		κ=0.899		κ=0.951	

Table 7: Comparison of various imaging techniques with HRCT for detecting ill-defined nodules.

Ill-defined nodules	HRCT		DECT 80 keV		DECT 140 keV		Mixed	
	No.	%	No.	%	No.	%	No.	%
Negative	36	53.7	37	55.2	40	59.7	38	56.7
Positive	31	46.3	30	44.8	27	40.3	29	43.3
Total	67	100.0	67	100.0	67	100.0	67	100.0
+ve % of HRCT			96.8		87.1		93.5	
Significance			χ^2=63.09, *P*<0.001		χ^2=52.52, *P*<0.001		χ^2=59.38, *P*<0.001	
Agreement			κ=0.970		κ=0.879		κ=0.940	

Table 8: Comparison of various imaging techniques with HRCT for detecting calcified granuloma.

Calcified granuloma	HRCT		DECT 80 keV		DECT 140 keV		Mixed	
	No.	%	No.	%	No.	%	No.	%
Negative	42	62.7	42	62.7	47	70.1	44	65.7
Positive	25	37.3	25	37.3	20	29.9	23	34.3
Total	67	100.0	67	100.0	67	100.0	67	100.0
+ve % of HRCT			100.0		80.0		92.0	
Significance			χ^2=67.00, *P*<0.001		χ^2=47.90, *P*<0.001		χ^2=58.84, *P*<0.001	
Agreement			κ=1.000		κ=0.834		κ=0.935	

Descriptive statistical analysis, which included frequency, percentages, mean, standard deviation, and median, was used to characterize the data. Chi-square test was applied to check associations. $P < 0.05$ was considered statistically significant.

Kappa statistics: Cohen's kappa coefficient was used to measures inter-rater agreement for qualitative items. It is generally thought to be a more robust measure than simple percent agreement calculation, as κ takes into account the possibility of the agreement occurring by chance.

On comparing the various imaging techniques (80, 140, and mixed) in DECT with HRCT for detecting lesions in lung, the maximum agreement of HRCT was found with DECT 80 keV followed by mixed and minimum agreement was found with DECT 140 keV.

Table 9: Comparison of various imaging techniques with HRCT for detecting fibrosis.

Fibrosis	HRCT		DECT 80 keV		DECT 140 keV		Mixed	
	No.	%	No.	%	No.	%	No.	%
Negative	47	70.1	48	71.6	50	74.6	49	73.1
Positive	20	29.9	19	28.4	17	25.4	18	26.9
Total	67	100.0	67	100.0	67	100.0	67	100.0
+ve % of HRCT			95.0		85.0		90.0	
Significance			χ^2=62.32, *P*<0.001		χ^2=53.53, *P*<0.001		χ^2=57.84, *P*<0.001	
Agreement			κ=0.964		κ=0.888		κ=0.927	

Table 10: Comparison of various imaging techniques with HRCT for detecting peribronchial thickening.

Peribronchial thickening	HRCT		DECT 80 keV		DECT 140 keV		Mixed	
	No.	%	No.	%	No.	%	No.	%
Negative	50	74.6	51	76.1	53	79.1	52	77.6
Positive	17	25.4	16	23.9	14	20.9	15	22.4
Total	67	100.0	67	100.0	67	100.0	67	100.0
+ve % of HRCT			94.1		82.4		88.2	
Significance			χ^2=61.82, *P*<0.001		χ^2=52.05, *P*<0.001		χ^2=56.84, *P*<0.001	
Agreement			κ=0.960		κ=0.874		κ=0.918	

RESULTS

On comparing the various imaging techniques with HRCT for detecting consolidation [Table 1], tree in bud pattern [Table 2], cavity [Table 3], ground-glass opacity [Table 4], tractional bronchiectasis [Table 5], atelectasis [Table 6], ill-defined nodules [Table 7], calcified granuloma [Table 8], fibrosis [Table 9], and peribronchial thickening [Table 10], the maximum agreement of HRCT was found with DECT 80 keV followed by mixed and minimum agreement was found with DECT 140 keV, as shown in Table 11. All the agreements were found to be highly significant ($P < 0.001$) [Figures 1-4].

In the right lung, it was observed that upper lobe has the maximum number of lesions as detected by HRCT 65.3% lesions, by DECT 80 keV 65.1% lesions, by DECT 140 keV 63.9% lesions, and by mixed 66.2% lesions.

Least number of lesions was found in lower lobe as detected by HRCT 6.2% lesions, by DECT 80 keV 6.0% lesions, by DECT 140 keV 5.9% lesions, and by mixed 5.4% lesions.

In the left lung, it was observed that upper lobe has the maximum number of lesions as detected by HRCT 93.8% lesions, by DECT 80 keV 94.0% lesions, by DECT 140 keV 93.7% lesions, and by mixed 94.6% lesions.

Remaining lesions were in lower lobe as detected by HRCT 6.2% lesions, by DECT 80 keV 6.0% lesions, by DECT 140 keV 6.3% lesions, and by mixed 5.4% lesions.

DISCUSSION

In 2016, an estimated 28 lakh cases occurred and 4.5 lakh people died due to TB. India also has over a million missed cases each year not notified, most of them not yet identified or unreportedly diagnosed or inadequately treated in the private sector.

The latest guidelines for diagnosis of adult chest TB are mainly based on examples of sputum microscopy for acid-fast bacilli (AFB). Chest radiograph (CXR) is used in sputum-negative patients who do not respond to antibiotics. Sputum smear results take several days while culture results need several weeks. This limits the diagnostic efficiency of these conventional approaches and frequently causes delays in isolating infectious patients. These tests also suffer from low sensitivity. Because of these limitations, imaging plays an important role in evaluation of chest TB (CTB) patients and CT is more sensitive than CXR in this regard. It is important to have imaging parameters and recommendations identified with India having a large burden of TB.[13,14]

The concept of DECT originated in the 1970s, including both dual-source and single-source configurations, made DECT feasible for routine clinical use.[15,16] With the increasing availability of CT systems capable of DECT, a growing variety of clinical applications, especially in the lung, has been reported.

Dual-energy computed tomography (DECT), based on a simultaneous acquisition at low and high kilo voltage, generates monochromatic reconstructions and material

density images, with spectral analysis of monochromatic images ranging from 40 keV up to 140 keV.

Low keV (i.e., <70 keV) images critically enhance iodine contrast, yet at the expanse of a significant increase of the image noise which could be deleterious at the lowest keV levels; therefore, a balance is needed between contrast and noise, and many studies have sought to determine that optimal monochromatic energy level.

In routine experience with DECT, we noticed a substantial change in lung parenchyma aspect when varying the keV. In our study, we hypothesize that a specific keV value could offer a better image quality for the depiction of lung parenchyma lesions.

In our study, after comparing the results of HRCT and DECT, the maximum agreement of HRCT was found with DECT 80 keV followed by mixed and minimum agreement was found with DECT 140 keV.

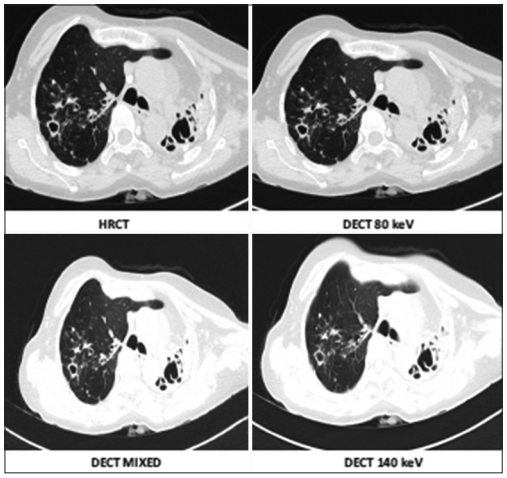

Figure 1: A 65-year-old man who presented with cough and weight loss with diagnosis of pulmonary tuberculosis. Axial high-resolution computed tomography (CT) and contrast-enhanced dual-energy CT (80 keV, mixed, and 140 keV) images showing cavity with surrounding nodules (few of these nodules are calcified) in the right lung and collapsed left lung with bronchiectatic changes and few calcified nodules. A large calcified lymph node is noted right paratracheal region.

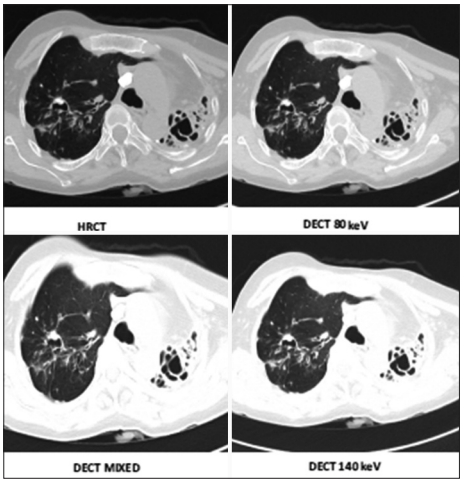

Figure 2: A 60-year-old man who presented with fever and cough with diagnosis of pulmonary tuberculosis. Axial high-resolution computed tomography (CT) and contrast-enhanced dual-energy CT (80 keV, mixed, and 140 keV) images showing cavity with a calcified foci within with surrounding nodules (few of these nodules are calcified), fibrosis in the right lung and collapse left lung with bronchiectatic changes and few calcified nodules. A large calcified lymph node is noted in the right paratracheal region.

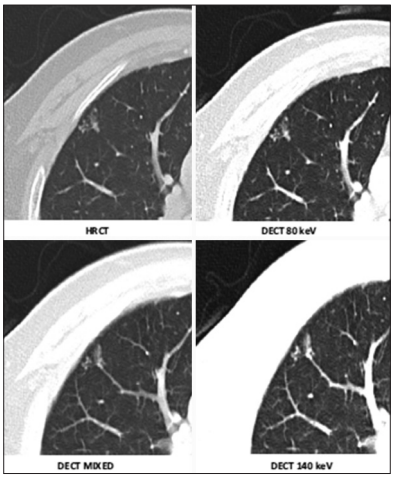

Figure 3: A 60-year-old man who presented with fever and cough with diagnosis of pulmonary tuberculosis. Axial high-resolution computed tomography (CT) and contrast-enhanced dual-energy CT (80 keV, mixed, and 140 keV) images showing tree in bud pattern.

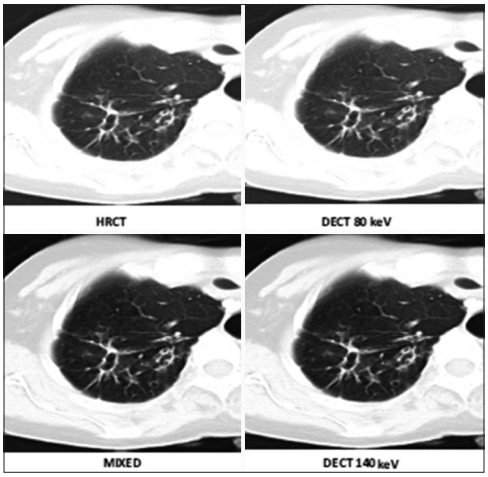

Figure 4: A 65-year-old woman who presented with fever cough and fatigue with diagnosis of pulmonary tuberculosis. Axial high-resolution computed tomography (CT) and contrast-enhanced dual-energy CT images showing bronchiectasis with peribronchial thickening. A calcified lymph node is noted in the right paratracheal region.

Table 11: Comparison of various imaging techniques with +ve % of HRCT.

Imaging techniques	DECT 80 keV	DECT 140 keV	Mixed
1. Consolidation	96.4	82.1	89.3
Agreement	κ=0.969	κ=0.843	κ=0.907
2. Tree in bud pattern	97.5	85.0	92.5
Agreement	κ=0.969	κ=0.820	κ=0.909
3. Cavity	100.0	85.2	92.6
Agreement	κ=1.000	κ=0.873	κ=0.937
4. GGO	95.5	86.4	95.5
Agreement	κ=0.966	κ=0.895	κ=0.966
5. Traction bronchiectasis	94.7	89.5	89.5
Agreement	κ=0.963	κ=0.924	κ=0.924
6. Atelectasis	100.0	84.6	92.3
Agreement	κ=1.000	κ=0.899	κ=0.951
7. Ill-defined nodules	96.8	87.1	93.5
Agreement	κ=0.970	κ=0.879	κ=0.940
8. Calcified granuloma	100.0	80.0	92.0
Agreement	κ=1.000	κ=0.834	κ=0.935
9. Peribronchial Thickening	94.1	82.4	88.2
Agreement	κ=0.960	κ=0.874	κ=0.918
10. Fibrosis	95.0	85.0	90.0
Agreement	κ=0.964	κ=0.888	κ=0.927

All the agreements were found to be highly significant ($P < 0.001$)

In our study, it was observed that with reference to HRCT, the sensitivity and specificity were maximum for DECT 80 keV and minimum for DECT 140 keV. The diagnostic accuracy was maximum for DECT 80 keV and mixed and minimum for DECT 140 keV.

The findings of the present study support that 80 keV is optimal monochromatic energy level for the qualitative analysis of lung parenchyma in thoracic DECT. DECT is a useful tool in the diagnosis and management of TB.

In another study, Johnson *et al*.[17] observed that dual-energy CT is more tissue specific in CT and can improve the assessment of vascular diseases. In a study conducted by Kawai *et al*. (2011),[18] they found that dual-energy computed tomography can evaluate contrast enhancement of GGA lesions.

CONCLUSION

The study concluded that DECT is a powerful and reliable investigation in the diagnosis of TB, when other means of diagnosis (e.g., culture and BAL) fail to settle the matter, are not available or time consuming. Routine chest DECT in pulmonary TB could be optimal for lung parenchyma with the sole analysis of the 80 keV monochromatic reconstructions among 80 keV, mixed, and 140 keV monochromatic reconstructions in lung parenchyma window settings, resulting in a faster and better analysis with reduced radiation dose when compared with HRCT.

Declaration of patient consent

The Institutional Review Board (IRB) permission obtained for the study.

Financial support and sponsorship

Nil.

Conflicts of interest

There are no conflicts of interest.

REFERENCES

1. Cegielski JP, Chin DP, Espinal MA, Frieden TR, Cruz RR, Talbot EA, *et al*. The global tuberculosis situation: Progress and problems in the 20th century, prospects for the 21st century. Infect Dis Clin North Am 2002;16:1-58.
2. Corbett EL, Watt CJ, Walker N, Maher D, Williams BG, Raviglione MC, *et al*. The growing burden of tuberculosis: Global trends and interactions with the HIV epidemic. Arch Intern Med 2003;163:1009-21.
3. Tufariello JM, Chan J, Flynn JL. Latent tuberculosis: Mechanisms of host and bacillus that contribute to persistent infection. Lancet Infect Dis 2003;3:578-90.
4. World Health Organization. Programmes and Projects. Tuberculosis. The Stop TB Strategy. Geneva: World Health Organization; 2018. Available from: http://www.who.int/tb/strategy/en. [Last accessed on 2018 May 21].
5. WHO Global Tuberculosis Report 2013; 2018. Available from: http://www.who.int/tb. [Last accessed on 2018 Aug 06].

6. TBC India: Tuberculosis Key Facts; 2018. Available from: http://www.tbcindia.nic.in/key.html. [Last accessed on 2018 Aug 16].
7. Im JG, Itoh H, Shim YS, Lee JH, Ahn J, Han MC, *et al*. Pulmonary tuberculosis: CT findings: Early active disease and sequential change with antituberculous therapy. Radiology 1993;186:653-60.
8. Woodring JH, Vandiviere HM, Fried AM, Dillon ML, Williams TD, Melvin IG. Update: The radiographic features of pulmonary tuberculosis. AJR Am J Roentgenol 1986;146:497-506.
9. Chae EJ, Seo JB, Jang YM, Krauss B, Lee CW, Lee HJ, *et al*. Dual-energy CT for assessment of the severity of acute pulmonary embolism: Pulmonary perfusion defect score compared with CT angiographic obstruction score and right ventricular/left ventricular diameterratio. AJR Am J Roentgenol 2010;194:604-10.
10. McGuinness G, Naidich DP, Jagirdar J, Leitman B, McCauley DI. High-resolution CT findings in miliary lung disease. J Comput Assist Tomogr 1992;16:384-90.
11. Kim WS, Moon WK, Kim IO, Lee HJ, Im JG, Yeon KM, *et al*. Pulmonary tuberculosis in children: Evaluation with CT. AJR Am J Roentgenol 1997;168:1005-9.
12. Pastores SM, Naidich DP, Aranda CP, McGuinnes G, Rom WN. Intrathoracic adenopathy associated with pulmonary tuberculosis in patients with human immunodeficiency virus infection. Chest 1993;103:1433-7.
13. Bhalla A, Goyal A, Guleria R, Gupta A. Chest tuberculosis: Radiological review and imaging recommendations. Indian J Radiol Imaging 2015;25:213-25.
14. Ohana M, Labani A, Jeung MY, Roy C, Strasbourg FR. What is the Optimal Monochromatic keV Level for Lung Parenchyma Analysis in Spectral CT? A Qualitative Study on 50 Patients, ECR No. B-0582; 2016.
15. Ko JP, Brandman S, Stember J, Naidich DP. Dual-energy computed tomography: Concepts, performance, and thoracic applications. J Thorac Imaging 2012;27:7-22.
16. Kaza RK, Platt JF, Cohan RH, Caoili EM, AlHawary MM, Wasnik A. Dual-energy CT with single-and dual-source scanners: Current applications in evaluating the genitourinary tract. Radiographics 2012;32:353-69.
17. Kawai T, Shibamoto Y, Hara M, Arakawa T, Nagai K, Ohashi K. Can dual-energy CT evaluate contrast enhancement of ground-glass attenuation? Phantom and preliminary clinical studies. Acad Radiol 2011;18:682-9.
18. Johnson TR. Twin energy CT: Scientific proof and clinical application AL Mohammad MA. Dual Energy CT-A diagnostic boon. Radiol Diagn Imaging 2010;2:5-6. Available from: https://www.oatext.com/pdf/RDI-2-125.pdf [Last accessed on 2020 Jul 04].

How to cite this article: Khan AU, Khanduri S, Tarin Z, Abbas SZ, Husain M, Singh A, *et al*. Dual-Energy Computed Tomography Lung in patients of Pulmonary Tuberculosis. J Clin Imaging Sci 2020;10:39.